Energy Conversion and Management 172 (2018) 105–118

Contents lists available at ScienceDirect

Energy Conversion and Management

journal homepage: www.elsevier.com/locate/enconman

Thermodynamic and economic assessment of a novel CCHP integrated system taking biomass, natural gas and geothermal energy as co-feeds

Xiaofeng Zhang[a,*], Xiaobo Liu[a], Xiaoqin Sun[a], Changwei Jiang[a], Hongqiang Li[b,*], Quanbin Song[a], Jing Zeng[a], Guoqiang Zhang[b]

[a] College of Energy and Power Engineering, Changsha University of Science and Technology, Changsha, Hunan 410114, China
[b] College of Civil Engineering, National Center for International Research Collaboration in Building Safety and Environment, Hunan University, Changsha, Hunan 410082, China

ARTICLE INFO

Keywords:
Combined cooling heating and power (CCHP) system
Co-firing
Biomass gasification
Ground source heat pump (GSHP)
Natural gas

ABSTRACT

The combined cooling, heating and power (CCHP) system based on biomass, geothermal energy and fossil energy contributes to less fossil fuel-dependent, alleviate the climate change and improve the flexibility of integrated system. Therefore, this paper presents a novel combined cooling, heating and power (CCHP) system based on biomass, natural gas and geothermal energy. The CCHP system consists of an air-biomass gasification subsystem, steam turbine electricity generation subsystem, gas turbine electricity generation subsystem, waste heat utilization subsystem and ground source heat pump subsystem. The thermodynamic and economic analysis of proposed system are investigated, and the influences of some key operating parameters (gas mass ratio and flue gas split ratio) and economic factors (such as biomass and natural gas price, interest rate, operating time coefficient and service life) on integrated system performances are also carried out. The results indicate that the introduction of natural gas contributes to improve the overall energy efficiency of proposed CCHP system and reduce the levelized cost of energy significantly. In the case study (gas mass ratio: 0.5, flue gas split ratio: 0.5), the overall energy efficiency and electricity generation efficiency of CCHP system can be reached at about 97.05% and 30.89%, respectively; the levelized cost of energy is 0.0315 $/kWh. The proposed system provides a new way for utilization of renewable energy and fossil fuels based poly-generation system, which is a promising approach for the utilization of biomass, natural gas and geothermal energy in the rural of China.

1. Introduction

With the rapid development of global society and economy, energy issues are gaining increasing attention. According to the statistics of International Energy Agency (IEA), the world energy demand rose by 2.1% in 2017, more than twice the rate of 2016. The fossil fuels, such as oil, natural gas and coal, accounted for about 81% of the total energy demand in 2017. Accordingly, the world energy-related carbon dioxide emissions increased, which reached a historical high of 32.5 gigatonnes in 2017 [1]. Besides that, the utilization of fossil fuels also results in the environment pollution and ecological destruction. Hence, it is imperative to consider the clean and efficient energy as the alternatives, and the renewable energy is an attractive option. In order to further improve energy efficiency and realize the energy cascade utilization, the selection of energy supply system is also important.

In recent years, the distributed energy system has been widely developed due to their high energy efficiency, environmental protection and high reliability [2]. There are many different structures considering the distinct energy inputs and outputs, such as combined heat and power (CHP) system [3], combined cooling, heating and power (CCHP) system [4], trigeneration system [5] and polygeneration system [6]. Currently, more and more renewable energy is adopted in the distributed energy system so as to decrease the fossil fuels-dependent and enlarge the applications of renewable energy. The related investigations have been carried out from different issues, such as the analysis of thermodynamic performance [7], economic feasibility [8], the optimization of system structure and operation [9,10].

Among the above renewable energy resources, biomass and geothermal energy have attracted more attention for their unique advantages [11]. As a carbon neutral resource, biomass can efficiently reduce the carbon dioxide (CO_2) emission compared with fossil fuels [12]. Through different utilization methods (combustion, fermentation, pyrolysis, gasification), the biomass can be converted into various products directly or indirectly: synthetic gas [13], methanol [14], heat

* Corresponding authors.
E-mail addresses: xiaofengzhang@csust.edu.cn (X. Zhang), lhq@hnu.edu.cn (H. Li).

https://doi.org/10.1016/j.enconman.2018.07.002
Received 28 May 2018; Received in revised form 22 June 2018; Accepted 2 July 2018
Available online 10 July 2018
0196-8904/ © 2018 Elsevier Ltd. All rights reserved.

Nomenclature

Abbreviations

ANN	artificial neural network
ATC	annual total cost
CCHP	combined cooling, heating and power
CCP	combined cooling and power
CGE	cold gas efficiency
CHP	combined heating and power
COE	cost of electricity
COH	cost of heat
COP	coefficient of performance
ER	equivalence ratio
GCU	gas conditioning unit
GMR	gas mass ratio
GSHP	ground source heat pump
GT	gas turbine cycle
HX	heat exchanger
ICE	internal combustion engine
LCOE	levelized cost of energy
LHV	lower heating value
MGT	micro gas turbine
NG	natural gas
O&M	operation & maintenance
ORC	organic rankine cycle
SR	split ratio
ST	steam turbine cycle

Symbols

A	heat transfer area (m^2)
C	investment cost of component ($)
c	fuel price ($/ton, $/$m^3$)
c_p	specific heat capacity (kJ/(kmol·K))
d	service life (year)
E	electricity (kW)
h	specific enthalpy (kJ/kg)
I	capital recovery factor
K	heat transfer coefficient (W/(m^2·K))
m	mass flow rate (kg/h)
n	poly-tropic exponent
P	pressure (Pa)
Q	heat (kW)
q	specific heat (kW/kg)
R	universal gas constant (kJ/kmol·K)
r	interest rate (%)
T	temperature (°C)
t	annual operation hour (h)
V	volume flow rate (Nm^3/h)
w	specific electricity (kW/kg)
η	efficiency (%)

Subscripts

C	cooling
c	condenser
e	evaporator
H	heating
mix	mixture gas
wf	working fluid

[3], power [15], etc. At the same time, the ground source heat pump (GSHP) is usually adopted to utilize the geothermal energy [16], which has the stable heat source from the Earth's interior and not influenced by season and weather conditions. Some researchers have studied the integrated energy system base on biomass and geothermal energy. Malik et al. [17] assessed the energetic and exergetic performances of a biomass combustion and geothermal power generation based multi-generation system, providing electricity, hot water, cooling, liquefied gas and hot drying air for residential buildings; and the influences of key parameters on system performances are also investigated. Patarau et al. [18] presented a techno-economic analysis of a hybrid renewable energy system for a vegetable greenhouse in Oradea region, Romania. The hybrid energy system mainly consists of: solar panels, a geothermal generator and a biogas generator. Seethamraju et al. [19] integrated a biomass combustor with an existing geothermal electricity generation plant, utilized the combustion heat from biomass combustor to further heat the geothermal steam. In order to select an optimal alternative, three different scenarios have been adopted to demonstrate the integration performances of different scenarios. Moret et al. [20] presented an appropriate methodology for urban energy systems combined with deep geothermal energy and woody biomass, and validated the model performance by an application case study in Switzerland. Lukawski et al. [21] studied a geothermal-biomass hybrid renewable energy system to achieve the Cornell's transformation energy plan, the proposed system adopted biomass boiler to generate the heat production and combined with geothermal energy and ORC to provide electricity. According to the above literature survey, the researches mainly concentrated on the energy power generation or CHP system integrated with biomass combustion and geothermal power generation, and rarely focused on biomass gasification and ground source heat pump (GSHP) based integrated energy system. To date, the authors have investigated a novel combine heating and power (CHP) system integrating with biomass and geothermal energy in terms of exergetic and exergoeconomic aspects [22]. Moreover, a multi-objective optimization model of the proposed system was investigated in order to obtain the optimal capacity and operation strategy [23]. Although the above CHP system provides a new way for biomass and geothermal based energy integration system, it has adjustability limitation to a certain extent and cannot meet the multiple load demands of users.

In addition, the biomass cannot meet the energy requirement of users throughout the whole year considering the low energy density and limited utilization efficiency. Therefore, some researchers proposed the concept of co-firing to alleviate the above problems. Fan et al. [24] investigated a biomass and coal co-feed chemical looping combustion for combined cooling, heating and power generation system from the perspective of thermodynamic and environmental assessment. Walter and Llagostera [25] analyzed the feasibility of co-fired combined-cycles utilizing sugarcane residues-derived gas and natural gas in terms of economic aspects, the authors compared with the current and middle term costs of combined cycle through calculating the capital, operation and maintenance costs. Wang et al. [26] studied the thermodynamic and exergoeconomic performances of a novel co-fired CCHP (combined cooling, heating and power) system taking natural gas and biomass product gas as co-feeds, the presented system mainly contains a gasifier, internal combustion engine (ICE), absorption chiller and heat exchangers. The results showed that the co-firing of natural gas and biogas can decrease the primary energy consumptions considering the high energetic and exergetic efficiencies. Agbor et al. [27] presented a techno-economic model to analyze the technical potential and economic feasibility of 60 scenarios for co-firing biomass with coal and natural gas, and the environmental performances are also determined. Fiaschi and Carta [28] analyzed a co-firing of natural gas and biomass-

derived gas in a gas turbine power generation plant, the characteristics lies in the re-utilization of CO_2 in exhaust gas. The conclusions indicated that the CO_2 removal levels are about 30–50% when the range of biomass co-firing stays in 10–30%. Nikpey et al. [29] conducted on an experimental evaluation of a commercial 100 kW micro gas turbine (MGT) at full and part loads, the experimental data showed that

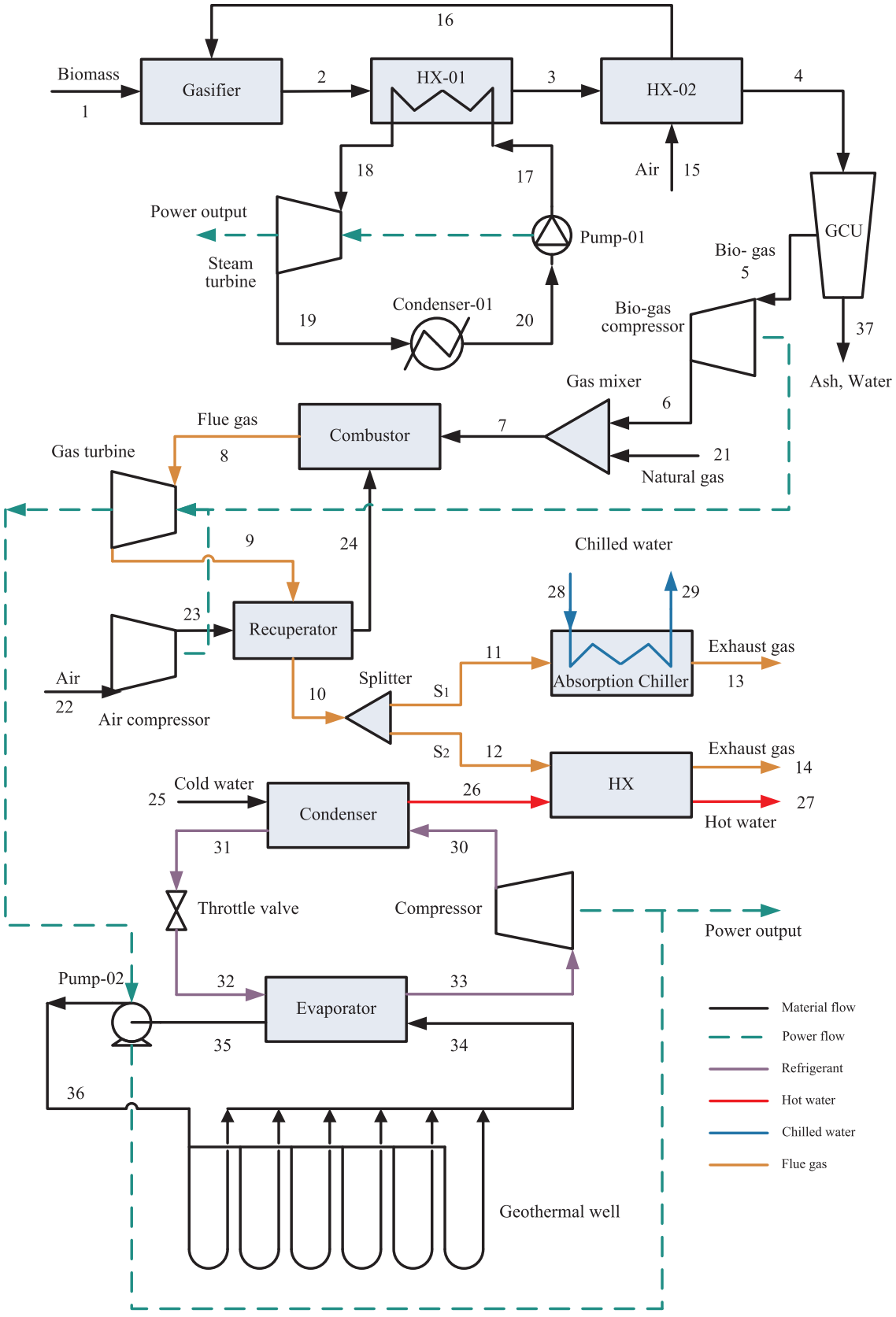

Fig. 1. Flow sheet of a co-firing biomass gasification gas and natural gas in CCHP system based on ground source heat pump.

mixture gas (natural gas and biogas) decreases CO_2 emissions significantly at full load operation. Moreover, the authors developed a artificial neural network (ANN) model to further simulate the performance of MGT. Kang et al. [30] investigated the thermodynamic and economic performances of biogas and natural gas co-firing in combined heat and power (CHP) system, the COE (cost of electricity) and COH (cost of heat) are calculated through the proposed method.

Thus, the main purpose of this study is to present a novel combined cooling, heating and power (CCHP) system utilizing biomass, natural gas and geothermal energy. The unique characteristics of proposed system lies in the following aspects: (i) the utilization of renewable energy resources (biomass and geothermal energy) can reduce the CO_2 emission and the consumption of fossil fuels; (ii) the natural gas is considered as the supplementary, which can improve the reliability of energy supply system; (iii) enhancing the flexibility of output products (electricity, heating and cooling) of energy system. The proposed CCHP system provides a novel way for the application of biomass and geothermal energy, especially for rural district where has an abundant biomass and shallow geothermal energy.

The rest of this work is organized as follows: Section 2 describes the configuration of novel combined cooling, heating and power (CCHP) system; Section 3 illustrates the system thermodynamic and economic evaluation method; Section 4 presents the results of thermodynamic and economic performances; Section 5 analyzes the effect characteristics of key operating and economic parameters; Section 6 summarizes the main conclusions of this work.

2. Configuration description of integrated system

The configuration of integrated CCHP system based on biomass, natural gas and geothermal energy is shown in Fig. 1. It is composed of an air-biomass gasification subsystem (gasifier, HX-01, HX-02, GCU), steam turbine electricity generation subsystem (HX-01, steam turbine, condenser 1, pump-01), gas turbine electricity generation subsystem (bio-gas compressor, gas mixer, air compressor, recuperator, combustor), waste heat utilization subsystem (splitter, absorption chiller, HX) and ground source heat pump subsystem (condenser, throttle valve, evaporator, compressor, pump-02, geothermal well).

For the air-biomass gasification subsystem, the biomass (stream 1) is fed into the gasifier with high temperature air (stream 16, 200 °C, 1 bar) for gasification reaction, and the air (stream 15, 25 °C, 1 bar) is preheated by the sensible heat of bio-gas (stream 3) in HX-02 (HX: heater exchanger). Considering the requirement of bio-gas utilization, the bio-gas (stream 4) is fed into the GCU (gas conditioning unit, which is mainly consisted of a cyclone and a scrubber) so as to remove the impurities and water (stream 37). In the steam turbine electricity generation subsystem, the Rankine cycle is proposed so as to further utilize the high temperature sensible heat of bio-gas. The pressured water

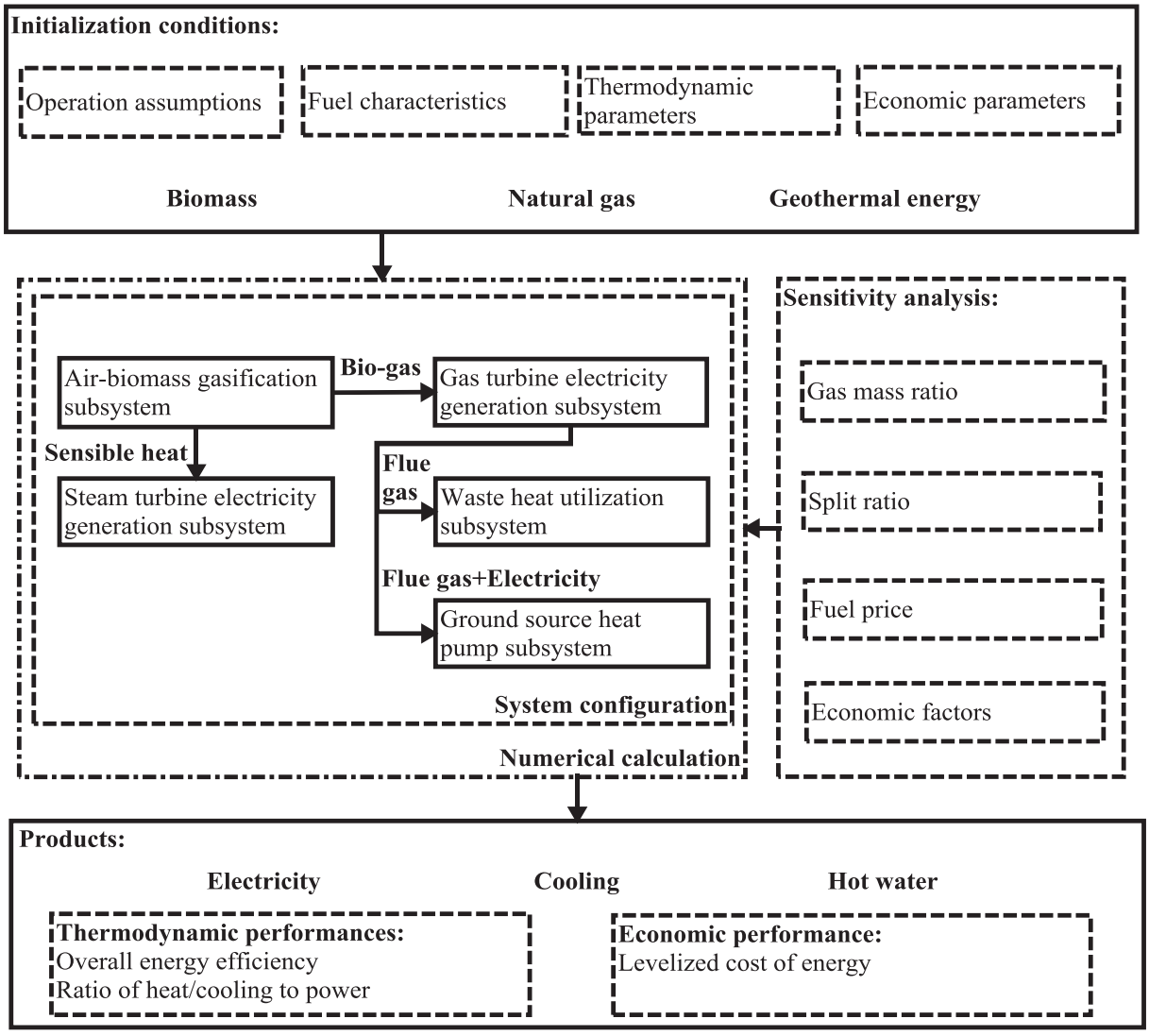

Fig. 2. Analysis process of proposed system.

Table 1
Characteristics of biomass material.

Items	Parameters				
Ultimate analysis (dry basis) (wt %)	Carbon	Hydrogen	Oxygen	Nitrogen	Sulfur
	39.78	4.97	40.02	0.46	0.20
Proximate analysis (dry basis) (wt %)	Volatile matter	Fixed carbon	Ash	Moisture	
	70.36	15.07	14.56	14.43	
HHV (MJ/kg)	14.144				

(stream 17, 55 bar) is superheated by the sensible heat of bio-gas (stream 2), then the high pressure superheated steam (stream 18, 500 °C, 55 bar) is set into steam turbine for power generation. After that, the exhaust steam (stream 19) is condensed in the condenser-01 and then pumped into the pump-01, which completes the whole thermodynamic cycle.

In the gas turbine electricity generation subsystem, the high pressured bio-gas (stream 6) is mixed with the natural gas (stream 21), and the mixture gas (stream 7) is combusted with the high pressure and temperature air (stream 24) in the combustor. The flue gas (stream 8) drives the gas turbine to generate the electricity, and then heats the air (stream 23) derived from the air compressor. For the waste heat utilization subsystem, the flue gas (stream 10) is separated into two streams: the flue gas 11 follows into absorption chiller to generate the chilled water (stream 29, 7 °C); The flue gas 12 follows into HX to reheat the warm water (stream 26, 39 °C), which generates the required hot water (stream 27, 55 °C).

In the ground source heat pump (GSHP) subsystem, the refrigerant (stream 30, R22) releases the heat in condenser and heats the cold water (stream 25, 25 °C, 1 bar) to the specified temperature (stream 26, such as 39 °C). After throttling and reducing pressure in the throttle valve, the refrigerant (stream 32) in the evaporator absorbs the geothermal heat from the geothermal well and reaches at a saturated vapor state (stream 33); then the superheated refrigerant derived from compressor follows into the condenser and heats the cold water. Unlike the conventional distributed energy and ground source heat pump integrated system, the ground source heat pump in the proposed system just generates the warm water, in which the temperature of warm water is below to the temperature of hot water. Then the waste heat of flue gas is utilized to further reheat the warm water into the required temperature. These measures can improve the COP of ground source heat pump and the efficiency of flue gas heat exchanger.

3. System performance evaluation methodology

Fig. 2 shows the analysis procedure so as to further study the thermodynamic and economic performances of integrated system. Firstly, the proposed system are presented, and related input conditions such as assumptions, fuel properties, thermodynamic and economic factors, are illustrated in methodology. Secondly, the numerical calculation of system should be completed, which contributes to analyze the thermodynamic and economic performances subsequently. Finally, the sensitivity analysis of key operating factors, such as gas mass ratio, flue gas split ratio, fuel price and economic factors, are conducted.

3.1. Thermodynamic analysis

3.1.1. Air-biomass gasification subsystem

For the biomass gasification process, the gasification performance is greatly dependent on the gasifying agent. Due to the low cost and widely used in application scale, air is considered as the gasifying agent in proposed system. The equivalence ratio (ER) can be expressed as:

Table 2
Key operation parameters of air-biomass gasification subsystem.

Parameters	Value	Unit
Flow rate of biomass	700	kg/h
Flow rate of air	1110	kg/h
Equivalence ratio (ER)	0.35	–
Temperature of gasification	888	°C
Pressure of gasification	1	bar
Temperature of air	200	°C
Pressure of air	1	bar
Node temperature difference of heat exchangers (HX-01, HX-02)	≥20	°C

$$ER = \frac{actual\ \ air/biomass\ \ ratio}{stoichiometric\ \ air/biomass\ \ ratio} \quad (1)$$

Besides that, the related assumptions of gasification process are also needed:

- The process contains isothermal and steady state.
- Material particles are of uniform size and temperature.
- The bio-gas is mainly composed of CO, H_2, CO_2, N_2, H_2O, tar is not considerable.
- The ash contained in char is treated as inert material.

In order to model the biomass gasification process, the process simulator Aspen Plus based on thermodynamic equilibrium models is adopted [31], and the calculation model of biomass gasification is reference to the previous study [32]. In this work, the rice husk is selected as a feedstock material considering the abundant biomass resources derived from rice in rural district of southern China [33]. The characteristics of rice husk are shown in Table 1, and the key operation parameters of gasification process are listed in Table 2.

3.1.2. Steam turbine electricity generation subsystem

The working fluid, water, is utilized to absorb the high temperature sensible heat of bio-gas in HX-01. The absorbed heat of HX-01 can be determined as:

$$Q_{HX-01} = \dot{m}_{wf}(h_{18} - h_{17}) \quad (2)$$

where $h_{17}$and $h_{18}$is the specific enthalpies of working fluid at the inlet and outlet of HX-01, kJ/kg, respectively.

The net electricity from steam turbine cycle is:

$$E_{st} = \dot{m}_{wf}\eta_{generator}[(h_{18} - h_{19}) - (h_{17} - h_{20})] \quad (3)$$

where $h_{19}$is the specific enthalpy of working fluid outlet of steam turbine, kJ/kg; $h_{20}$is the specific enthalpy of working fluid at the inlet of pump-01, kJ/kg. The main operating parameters are presented in Table 3.

3.1.3. Gas turbine electricity generation subsystem

In order to increase the reliability of proposed system, the mixture gas of bio-gas and natural gas is utilized to generate electricity, to further analyze the relationship between biomass and natural gas, the

Table 3
Key operation parameters of steam turbine electricity generation subsystem.

Parameters	Value	Unit
Inlet temperature of steam turbine	500	°C
Inlet pressure of steam turbine	55	bar
Isentropic efficiency of steam turbine	0.87	–
Mechanical efficiency of steam turbine	0.99	–
Isentropic efficiency of pump-01	0.75	–
Mechanical efficiency of pump-01	0.99	–
Condensation temperature	42	°C
Condensation pressure	0.08	bar

gas mass ratio of natural gas to bio-gas is defined:

$$GMR = \frac{\dot{m}_{NG}}{\dot{m}_{bio\text{-}gas}} \times 100\% \quad (4)$$

where $\dot{m}_{NG}$is the mass flow rate of natural gas, kg/h; $\dot{m}_{bio\text{-}gas}$is the mass flow rate of bio-gas, kg/h.

The lower heating value (LHV) of the mixture gas can be expressed as:

$$LHV_{mix} = \frac{LHV_{bio-gas}\dot{m}_{bio-gas} + LHV_{NG}\dot{m}_{NG}}{\dot{m}_{bio-gas} + \dot{m}_{NG}} \times 100\% \quad (5)$$

where $LHV_{bio\text{-}gas}$is the lower heating value of bio-gas, kJ/kg; $LHV_{NG}$is the lower heating value of natural gas, kJ/kg. The key operating values of gas turbine electricity production subsystem are shown in Table 4.

3.1.4. Waste heat utilization subsystem

For the utilization of flue gas, a splitter is adopted to adjust the distribution of flue gas derived from gas turbine, which can improve the flexibility of integrated system. The split ratio is defined as the ratio of flue gas sent into absorption chiller to the total flue gas outlet of recuperator:

$$SR = \frac{S_1}{S_1 + S_2} \quad (6)$$

where S_1 is the mass flow rate of flue gas sent into absorption chiller kg/h; S_2 is the mass flow rate of flue gas sent into HX, kg/h. The key operating parameters of waste heat utilization subsystem are listed in Table 5.

3.1.5. Ground source heat pump subsystem

Considering the theoretical knowledge of heat pump, the coefficient of performance (COP) is greatly dependent on the outlet temperature of demand side and inlet temperature of ground source side. The evaporated temperature and condensed temperature of heat pump are calculated as [34]:

$$T_e = \frac{T_{out\text{-}e}e^{\frac{K_eA_e}{C_pm_e}} - T_{in\text{-}e}}{e^{\frac{K_eA_e}{C_pm_g}} - 1} \quad (7)$$

$$T_c = \frac{T_{out\text{-}c}e^{\frac{K_cA_c}{C_pm_d}} - T_{in\text{-}c}}{e^{\frac{K_cA_c}{C_pm_d}} - 1} \quad (8)$$

where T_e and T_c are the evaporated and condensed temperature of refrigerant in heat pump respectively, ˚C; $T_{out\text{-}c}$ and $T_{in\text{-}c}$ are the outlet and inlet temperature of demand side in condenser respectively, ˚C; $T_{out\text{-}e}$ and $T_{in\text{-}e}$ are the outlet and inlet temperature of ground source side in evaporator respectively, ˚C; K is the heat transfer coefficient, W/(m^2·K); A is the heat transfer area, m^2.

The power consumption of compressor and coefficient of performance (COP) can also be determined:

$$w = \frac{RT_e}{n-1}\left(1 - \left(\frac{P_c}{P_e}\right)^{n-1/n}\right) \quad (9)$$

$$COP = \frac{q}{w} \quad (10)$$

where $P_c$and $P_e$are the condensed and evaporated pressure respectively, Pa; $R$is the universal constant; $n$is the poly-tropic exponent; $q$is the heating generation per unit mass refrigerant in heat pump, kw/kg.

According to the previous studies of authors, the evaporated and condensed temperatures of refrigerant nonlinearly increase with increase in pressure. When the other parameters are constant, the COP of heat pump increases with decrease in outlet temperature of demand side in condenser. The temperature of hot water in this study is set as 55 ˚C, so a temperature below this value is considered (such as 39 ˚C). The related operating parameters of ground source heat pump subsystem are also presented in Table 6.

3.2. Economic analysis

Economic performance analysis contributes to understand the feasibility of proposed system. Based on the above thermodynamic investigation, the capital investment, operation and maintenance of system can be obtained. The annual total cost (ATC) is composed of the following parts: annual capital cost of components, annual fuel cost and operation & maintenance cost [35], which can be expressed as follows:

$$ATC = I\sum_{j=1}^{J} C_j + C_{O\&M,CCHP} + \sum_{i}^{t}(c_{bio}\cdot\dot{m}_{bio} + c_{NG}\cdot\dot{m}_{NG}) \quad (11)$$

where C is the investment cost of the components, which can be calculated by the related investment cost function in Appendix A, $; j is the number of components of proposed system; $C_{O\&M,CCHP}$ is the annual operation and maintenance costs of proposed system, it can be expressed as $C_{O\&M,CCHP} = \varphi\sum_{j=1}^{J} C_j$ [5,36], φ is the proportion of operation and maintenance, which is assumes 6% of the system investment cost of proposed system. c_{bio} and c_{NG} are the price of biomass and natural gas respectively ($/ton, $/m^3); t is the annual operation hours, h; $\dot{m}_{bio}$ and $\dot{m}_{NG}$ are the mass flow rate of biomass and natural gas, kg/h; I is the capital recovery factor, it can be calculated as:

$$I = \frac{r(1+r)^d}{(1+r)^d - 1} \quad (12)$$

where r is the interest rate, %; d is the service life of system, year. The investment cost of components and other economic parameters are listed in Table 7.

3.3. Performance evaluation criteria

Based on the thermodynamic analysis of biomass gasification process in Section 3.1.1, the cold gas efficiency is selected as the indicator for gasification performance, which can be defined as the ratio of output energy of bio-gas to input energy of biomass feedstock.

$$CGE_{bio\text{-}gas} = \frac{LHV_{bio\text{-}gas}\dot{m}_{bio\text{-}gas}}{LHV_{biomass}\dot{m}_{biomass}} \times 100\% \quad (13)$$

where $LHV_{bio\text{-}gas}$ is the lower heating value of bio-gas, kJ/kg; $LHV_{biomass}$ is the lower heating value of biomass, kJ/kg.

In the proposed system, the outputs are electricity, cooling and hot water. Therefore, the overall energy efficiency is considered to assess the whole thermodynamic performance of proposed system, which can be expressed as:

Table 4
Key operation parameters of gas turbine electricity generation subsystem.

Parameters	Value	Unit
Pressure of natural gas	14	bar
Gas mass ratio	0.5	–
Compression ratio of bio-gas compressor	13.5	–
Isentropic efficiency of bio-gas compressor	0.85	–
Mechanical efficiency of bio-gas compressor	0.99	–
Isentropic efficiency of air compressor	0.82	–
Mechanical efficiency of air compressor	0.99	–
Inlet temperature of gas turbine	1150	˚C
Expansion ratio of gas turbine	13.5	–
Isentropic efficiency of gas turbine	0.87	–
Mechanical efficiency of gas turbine	0.99	–
Temperature of preheated air in recuperator	500	˚C

Table 5
Key operation parameters of waste heat utilization subsystem.

Parameters	Value	Unit
Split ratio	0.5	–
COP of absorption chiller	1.2	–
Outlet temperature of chilled water	7	˚C
Inlet temperature of chilled water	12	˚C
Temperature of hot water	55	˚C
Node temperature difference of heat exchanger	≥20	˚C
Temperature of exhaust gas	150	˚C
Ambient temperature	25	˚C
Ambient pressure	1	bar

Table 6
Key operation parameters of ground source heat pump subsystem.

Items	Value	Unit
Critical temperature of Refrigerant (R22)	96.2	˚C
Critical pressure of Refrigerant (R22)	49.8	bar
Temperature of cold water	25	˚C
Temperature of warm water	39	˚C
Flow rate of refrigerant	48,500	kg/h
Outlet temperature of source water in geothermal well	12	˚C
Inlet temperature of source water in geothermal well	7	˚C
Logarithmic mean temperature difference of evaporator	4.2	˚C
Min temperature approach of condenser	7.9	˚C

Table 7
Related economic parameters of proposed system.

Items	Parameter	Value	Unit
Investment cost of component	Refer to Appendix A	–	$
Economic factors	Service life	20	year
	Interest rate	10	%
	Operation hours	7446	h
	Proportion of operation and maintenance	6	%
Fuel price	Biomass	57.2	$/ton
	Natural gas	0.528	$/m^3

$$\eta = \frac{Q_H + Q_C + E_{ST} + E_{GT}}{LHV_{biomass}\dot{m}_{biomass} + LHV_{NG}\dot{m}_{NG}} \times 100\% = \frac{Q_{CHP} + Q_{GSHP} + Q_C + E_{ST} + E_{GT}}{LHV_{biomass}\dot{m}_{biomass} + LHV_{NG}\dot{m}_{NG}} \times 100\% \quad (14)$$

where Q_H is the heating generation of proposed system, kW; Q_{CHP} is the heat obtained from gas turbine electricity generation subsystem, kW; Q_{GSHP} is the heat obtained from ground source heat pump subsystem, kW; Q_C is the cooling generation of absorption chiller, kW; E_{ST} and E_{GT} is the net electricity output generated by steam turbine cycle and gas turbine cycle, respectively, kW.

In order to compare the system performance between proposed system and separated generation system, energy saving rate (ESR) is adopted [37]. It can be defined as the ratio of primary energy reduction of proposed CCHP system compared with separated generation system to primary energy consumption of separated generation system.

$$ESR = \frac{F_{SP} - F_{CCHP}}{F_{SP}} \times 100\% = \left(1 - \frac{LHV_{biomass}\dot{m}_{biomass} + LHV_{NG}\dot{m}_{NG}}{\frac{E_{ST}+E_{GT}}{\eta_{SP,el}\cdot\eta_{SP,tr}} + \frac{Q_C}{COP_{SP,C}\cdot\eta_{SP,el}} + \frac{Q_H}{\eta_{SP,H}}}\right) \times 100\% \quad (15)$$

where F_{SP} is the fuel consumption of separated generation system, kW; F_{CCHP} is the fuel consumption of proposed system, kW; $\eta_{SP,el}$ is the electrical efficiency of the conventional power plant (35%), %; $\eta_{SP,tr}$ is the transmission efficiency of the conventional power plant (92%), %; $COP_{SP,C}$ is the COP of electrical refrigerator (3.5); $\eta_{SP,H}$ is the thermal efficiency of boiler (85%), %.

The levelized cost of energy (LCOE) is usually considered to evaluate the project economic performance, it can be defined as the ratio of annual project cost to production, such as electricity, cooling or heating [38,39]. Considering the distinct energy grade between electricity, heating and cooling, the equivalent electricity of heating and cooling can be calculated by the Carnot efficiency [40]. Therefore, the formulation of LCOE can be presented as follows:

$$LCOE = \frac{ATC/t}{Q_H(1-T_0/T_H) + Q_C(T_0/T_C - 1) + E_{ST} + E_{GT}} \quad (16)$$

where T_0 is the ambient temperature, ˚C; T_H is the mean temperature of hot water, ˚C; T_C is the mean temperature of chilled water, ˚C.

4. System performances investigation

To further illustrate the thermodynamic and economic performances, a case study is selected. The key input parameters are as follows: mass flow rate of biomass: 700 kg/h; mass flow rate of natural gas: 785 kg/h; gas mass ratio: 0.5; split ratio of flue gas: 0.5; temperature of warm water: 39 ˚C. After the numerical simulation of proposed system the thermodynamic performances can be calculated, and the related economic parameters also determined. Table 8 shows the properties of mixture gas, bio-gas and natural gas. In the simulation of biomass gasification process, the distribution of bio-gas composition is accorded with the typical bio-gas composition of air-biomass gasification process [31]. Therefore, the result of bio-gas composition is reliable. Besides that, it can be seen the introduction of natural gas increase the components of combustible gas and the lower heating value improves subsequently. This measure contributes to increase the input energy of prime mover (such gas turbine cycle in presented study).

After the numerical calculation, the thermodynamic parameters of each stream are obtained in Table 9. Moreover, the inputs, outputs and performances of proposed system are also illustrated in Table 10. The inputs are biomass, natural gas and geothermal energy, in which the natural gas dominates due to its high energy density. The steam turbine cycle is adopted to utilize the sensible heat of bio-gas, the generated electricity is about 140 kW, and the electricity can reach to 4469 kW in gas turbine cycle. Besides that, the compressor of ground source heat pump consumes a part of electricity, 449 kW, so as to generate warm water (39 ˚C). The COP of ground source heat pump is 5.71 when the temperature of warm water is set at 39 ˚C. The net power generated by proposed system is 4154 kW; the related electricity generation efficiency can reach to 30.89%. For the waste heat utilization, the warm water is reheated by a part of flue gas in HX, in which the cold water finally reaches the required temperature (55 ˚C). The heating output mainly consists of two parts: heat generated by flue gas in gas turbine cycle (2928 kW) and heat generated by ground source heat pump (2561 kW). On the other hand, another part of flue gas is considered as the heat source of absorption chiller, which produces about 3408 kW cooling load. The introduction of ground source heat pump improves the heating output, and the overall energy efficiency of proposed system reaches at 97.05%. Under the same outputs, the proposed CCHP system saves more primary energy than separated generation system, the energy saving rate (ESR) can be reached at 18.16%. Moreover, in order to evaluate the economic performance of proposed system the cost of products is determined by levelized cost of energy, the LCOE is

Table 8
Characteristics of mixture gas, bio-gas and natural gas.

Materials	Compositions (mol%)						LHV (MJ/kg)
	CH_4	CO	H_2	CO_2	N_2	H_2O	
Bio-gas	–	21.2	16.1	10.7	48.9	3.1	3.94
Natural gas	100	–	–	–	–	–	50.03
Mixture gas	44	11.9	9.0	5.9	27.4	1.7	19.30

Table 9
Thermodynamic parameters of state point in CCHP system[a].

State	Fluid type	Pressure (bar)	Temperature (°C)	Mass flow rate (kg/h)
1	Biomass	1	25	700
2	Bio-gas	1	888	1776
3	Bio-gas	1	284	1776
4	Bio-gas	1	197	1776
5	Bio-gas	1	25	1571
6	Bio-gas	13.5	375	1571
7	Mixture gas	13.5	201	2356
8	Flue gas	13.5	1150	55,669
9	Flue gas	1.05	586	55,669
10	Flue gas	1.05	495	55,669
11	Flue gas	1.05	495	27,834
12	Flue gas	1.05	495	27,834
13	Flue gas	1.05	150	27,834
14	Flue gas	1.05	150	27,834
15	Air	1	25	1110
16	Air	1	200	1110
17	Water	55	41.5	450
18	Steam	55	500	450
19	Steam	0.08	41.5	450
20	Water	0.08	41.5	450
21	Natural gas	14	25	785
22	Air	1	25	53,313
23	Air	13.5	400	53,313
24	Air	13.5	500	53,313
25	Cold water	1	25	157,840
26	Water	1	39	157,840
27	Water	1	55	157,840
28	Chilled water	1	12	670,351
29	Chilled water	1	7	670,351
30	R22	16.9	65	48,500
31	R22	16.9	45.5	48,500
32	R22	5.5	4.8	48,500
33	R22	5.5	4.8	48,500
34	Water	1	12	367,390
35	Water	1	7	367,390
36	Water	1.5	7	367,390
37	Ash, water	1	25	205

[a] For the biomass gasifier, the biomass preheating is modeled so as to reduce the moisture content of biomass, therefore the mass flow rate of bio-gas (stream 2) is below to the inputs of gasifier.

0.0315 $/kWh.

5. Discussion

5.1. The influence of gas mass ratio on input parameters between biomass and natural gas

In order to investigate the thermodynamic performance of integrated system, the input energy of biomass is determined to constant, 2538 kW. By adjusting the mass flow rate of natural gas, the different gas mass ratio can be obtained. Fig. 3 presents the variations of related input parameters under different gas mass ratio. It can be seen from the picture that the mass flow rate of natural gas gradually increases with the increase in gas mass ratio (GMR). And the energy ratio (the ratio of input energy of natural gas to the input energy of biomass) subsequently increases when the input energy of natural gas rises. Furthermore, the lower heating value (LHV) of mixture gas increases with the increase in gas mass ratio, and the distinct difference of LHV between natural gas and bio-gas naturally results in a decrease in LHV of mixture gas. When the gas mass ratio is 0, that is the pure bio-gas, the LHV of mixture gas is 3.94 MJ/kg, while it can be reached at 26.98 MJ/kg at the gas mass ratio of 1.

5.2. The influence of split ratio and gas mass ratio on electricity output

Fig. 4 shows the effects of split ratio and gas mass ratio on electricity output of proposed system. Considering the power output derived from steam turbine cycle is constant, the variations are mainly dependent on the gas turbine electricity generation subsystem. As is shown in the picture, the electricity output increases with the increasing of gas mass ratio. It can be explained that the energy density of mixture gas increases when the gas mass ratio rises, more and more mixture gas is combusted in combustor and more electricity produced consequently. At the same time, the electricity grows by 11 times approximately due to the high LHV of natural gas as Fig. 3 depicted. In addition, the electricity output also increases with the increase in flue gas split ratio (SR), while the variation range of electricity output gradually rises. When the split ratio increases, more and more flue gas derived from recuperator is sent into the absorption chiller for generating cooling. The heating, that is hot water, will decrease, and the power consumption of compressor in ground source heat pump (GSHP) decreases accordingly, therefore the electricity output of proposed system rises.

Table 10
Performance calculation results.

NO.	Item	Value	Unit
Input			
1	Biomass	2538	kW
2	Natural gas	10,909	kW
3	Heat from soil	2137	kW
4	Temperature of warm water	39	°C
5	Mass flow rate of cold water	157,841	kg/h
6	Mass flow rate of refrigerant	48,500	kg/h
Output			
7	Electricity generation from steam turbine cycle	140	kW
8	Electricity generation from gas turbine cycle	4469	kW
9	Electricity consumed by GSHP	449	kW
10	Net power output	4154	kW
11	Cooling output	3408	kW
12	Heat generated by gas turbine cycle	2928	kW
13	Heat generated by GSHP	2561	kW
14	Power consumption per unit refrigerant	33.3	kJ
15	Pressure ratio of GSHP	3.07	–
System performance			
16	Overall energy efficiency	97.05	%
17	Cold gas efficiency	67.75	%
18	Electricity generation efficiency	30.89	%
19	Levelized cost of energy	0.0315	$/kWh
20	COP of GSHP	5.71	–
21	Ratio of heat to power	1.32	–
22	Ratio of cooling to power	0.82	–
23	Energy saving rate	18.16	%
24	Annual total cost	$1.09 * 10^6$	$

5.3. The influence of split ratio and gas mass ratio on heating output

Fig. 5 illustrates the variations of heating output under different split ratio and gas mass ratio. With the increase in gas mass ratio, the mass flow rate of flue gas rises in the HX when the split ratio is kept constant, and the heat released in HX will increase. Due to the constant temperature of exhaust gas (150 °C) and hot water (55 °C) existed from HX, the flow rate of hot water will increase. Accordingly, the heating output also rises. Moreover, when the gas mass ratio is constant, the heating output of proposed system decreases with the increasing of flue gas split ratio. As the above analysis in Section 5.2, the flow rate of flue gas utilized to heat hot water is reduced with the increase in split ratio. Besides that, the decreasing increment of heating output rises. This phenomenon can be illustrated that: When the gas mass ratio is high the input energy of mixture gas reaches at maximum value, the flow rate of flue gas also reaches a maximum and vice verse. For example, when the gas mass ratio is 0, the heating output varies from 1596.2 kW to 0 kW with the increase in split ratio from 0 to 1.0; while the heating output decreases from 20361.6 kW to 0 kW at gas mass ratio of 1.0.

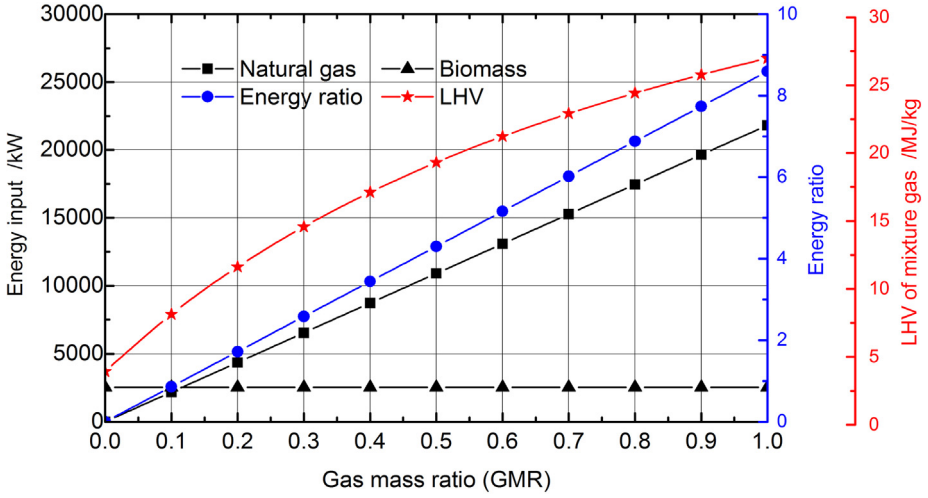

Fig. 3. The variations of input parameters under different gas mass ratio (GMR).

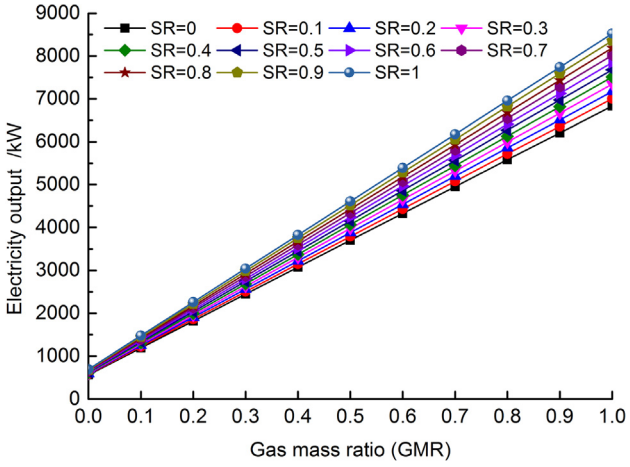

Fig. 4. The influences of split ratio and gas mass ratio on electricity output of proposed system.

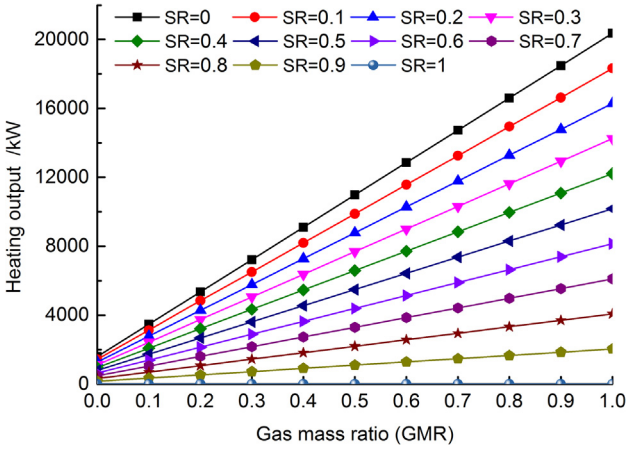

Fig. 5. The influences of split ratio and gas mass ratio on heating output of proposed system.

5.4. The influence of split ratio and gas mass ratio on cooling output

The effects of split ratio and gas mass ratio on cooling output of proposed system are depicted in Fig. 6. The cooling output increases with the increase in gas mass ratio, which is consistent with the variation of heating output under different gas mass ratio and the explanation is also similar to it. More and more natural gas is sent into combustor to generating electricity, the flow rate of flue gas sharply increases. Hence, the heating and cooling output rise subsequently. On the contrary, the cooling output increases with increasing of flue gas split ratio. It can be explained that: more and more flue gas will be utilized in absorption chiller when split ratio varies from 0 to 1.0, which increases the input waste heat of absorption chiller and cooling output accordingly. Similarly, the increasing range of cooling output becomes more and more noticeable with the increase in gas mass ratio. In addition, the variation of cooling output in this picture is below to the variation of heating output in Fig. 5, which can be attributed to the utilization of ground source heat pump. Although, the ground source heat pump subsystem consumes a part of electricity derived from proposed system, it transfers a part of heat derived from soil into hot water. This measure improves the growth of heating output.

5.5. The influence of split ratio and gas mass ratio on the ratio of heating/cooling to power

The ratio of heating/cooling to power is a significant parameter, which can not only determine the output proportion between heat/cooling and power, but also evaluate the performances of proposed system considering both supply and demand sides. Hence, it is necessary to analyze the variations of ratio of heating /cooling to power

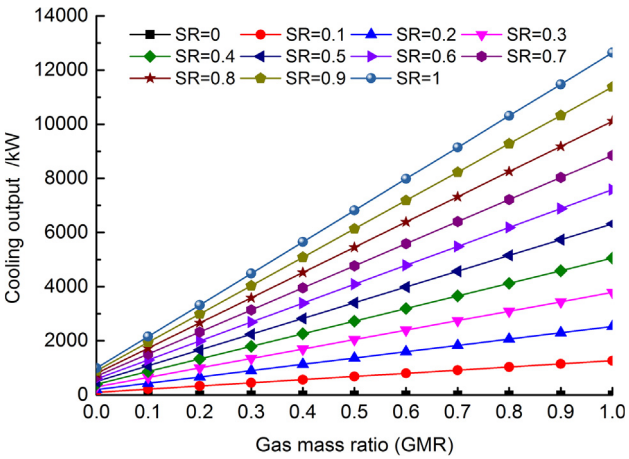

Fig. 6. The influences of split ratio and gas mass ratio on cooling output of proposed system.

under different gas mass ratio and flue gas split ratio. Fig. 7 reflects the effects of gas mass ratio and split ratio on ratio of heating to power. The ratio of heating to power decreases with the increasing of split ratio obviously, while slowly increases with the increasing of gas mass ratio. The above phenomenon can be explained as follows: on the one hand, the flow rate of flue gas in HX decreases with the increase in split ratio, and the heating output decreases subsequently; on the other hand, the electricity output increases with the increase in split ratio. Therefore, the ratio of heating to power reduces. Besides that the electricity and heating output all increase with the increase in gas mass ratio, the comprehensive effects results in an increase of ratio of heating to power not obviously. Fig. 8 presents the effects of gas mass ratio and split ratio on the ratio of cooling to power. Unlike the variations in Fig. 7, the ratio of cooling to power significantly increases with the increase in split ratio and slowly increases with the increase in gas mass ratio. Moreover, it can be observed from both Figs. 7 and 8 that the variation range of ratio of heat to power is higher than that of ratio of cooling to power. The main reason is as follows: the introduction of ground source heat pump converts apart of electricity generated by proposed system and geothermal energy into the heating output.

5.6. The influence of split ratio and gas mass ratio on overall energy efficiency

Fig. 9 displays the variations of overall energy efficiency of proposed system under different split ratio and gas mass ratio. When the flue gas split ratio keeps constant, the overall energy efficiency gradually increases. Particularly, the overall energy efficiency nonlinearly increases with the increase in gas mass ratio from 0 to 0.4; and then the increasing range is not obvious, which is below to 1%. The variation of overall energy efficiency is consistent with the variation of LHV in mixture gas depicted in Fig. 3. Although more electricity will be produced from gas turbine electricity generation subsystem with the increase in gas mass ratio, more electricity consumed by compressor in GSHP owing to the increase in flue gas flow rate. Hence, the increasing range gradually decreases when the gas mass ratio rises. From the above analysis, it can be concluded that the gas mass ratio is not the more the better, that is, the overall energy efficiency can reach at a good value when the gas mass ratio increases from 0 to 0.4. In addition, the overall energy efficiency decreases straightly with the increasing in flue gas split ratio. The introduction of ground source heat pump improves the heating output, which is higher than the cooling output. Despite the cooling output increases with the increase in split ratio, the increasing range is below to the decreasing range of heating output, which results in the decrease of whole output.

5.7. The influence of fuel prices on levelized cost of energy

According to Eq. (16), the variations of levelized cost of energy under different biomass price and gas mass ratio are concluded in Fig. 10. Considering the variations of some factors, such as biomass densification technology, labor cost, transportation cost, biomass collection radius, the biomass price varies. Moreover, the fluctuations of market price also affect the biomass price. Therefore, the benchmark price of biomass is set as 57.2 $/ton, which varies from −25% to +25% of the basic price with a 5% interval. It can be seen from this picture that the levelized cost of energy decreases exponentially with the increasing of gas mass ratio. The variation range of levelized cost of energy gradually decreases at the beginning of gas mass ratio of 0.4, and the purple zone dominates in the picture, which is below to 0.337 $/kWh. The introduction of natural gas, on the one hand results in the increase of investment cost of component and the fuel cost; on the other hand improves the outputs of products. Since the growth rate of total cost is lower than that of outputs, the overall results: the levelized cost of energy obviously decreases. In addition, the increase of biomass price results in the increasing of levelized cost of energy. When the gas mass ratio stays in a low value the levelized cost of energy increases significantly, conversely, the variations of levelized cost of energy are not obvious at high value of gas mass ratio.

Fig. 11 shows the effects of natural gas price and gas mass ratio on levelized cost of energy. The basic price of natural gas is 0.528 $/m^3, which varies from −25% to +25% of the benchmark price with a 5% interval. When the natural gas is constant, the variations of levelized cost of energy under different gas mass ratio are consistent with Fig. 10, that is, the levelized cost of energy increases non-linearly with the increase in gas mass ratio. In addition, unlike the variations of levelized cost of energy at different biomass prices, the effects of natural gas price on levelized cost of energy are less although the variations of levelized cost of energy shows an increasing trend.

5.8. The sensitivity analysis of levelized cost of energy under different economic factors

The sensitivity analysis contributes to analyze the influences of some economic factors (such as interest rate, operating time coefficient and service life) on product cost, levelized cost of energy. Fig. 12 illustrates the effects of interest rate and gas mass ratio on levelized cost of energy, the levelized cost of energy increases with the increasing of interest rate. It can be explained that, the capital recovery factor increases when the interest rate varies from 4% to 14% and the annual total cost of proposed system also increases. Therefore, the levelized cost of energy rises since the outputs of products are constant. Meanwhile, the levelized cost of energy increases obviously at the low value of gas mass ratio and varies slightly at the high value of gas mass ratio.

The effects of operating time coefficient and gas mass ratio on levelized cost of energy are presented in Fig. 13. The operating time coefficient is the ratio of actual operation hours to the hours of whole year (8760 h), the basic operation hours are 7446 h in this study (operating time coefficient: 0.85). The levelized cost of energy decreases nonlinearly with the increase in operating time coefficient. When the gas mass ratio keeps constant, the annual total cost of proposed system decreases with the increasing of operating time coefficient, which results in the decrease of levelized cost of energy. Moreover, the variation range of levelized cost of energy caused by operating time coefficient is higher than others economic factors. The maximum value of levelized cost of energy can reach at 0.1289 $/kWh, a considerable number of values exceed 0.08 $/kWh.

Fig. 14 shows the variations of levelized cost of energy under different service life and gas mass ratio. It can be seen from the picture that the levelized cost of energy decreases with the increasing of service life. Similarly, as the explanation in Fig. 13, the capital recovery factor

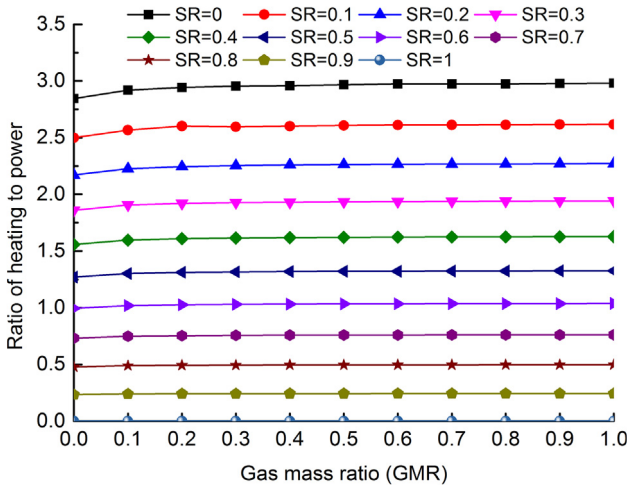

Fig. 7. The influences of split ratio and gas mass ratio on the ratio of heating to power.

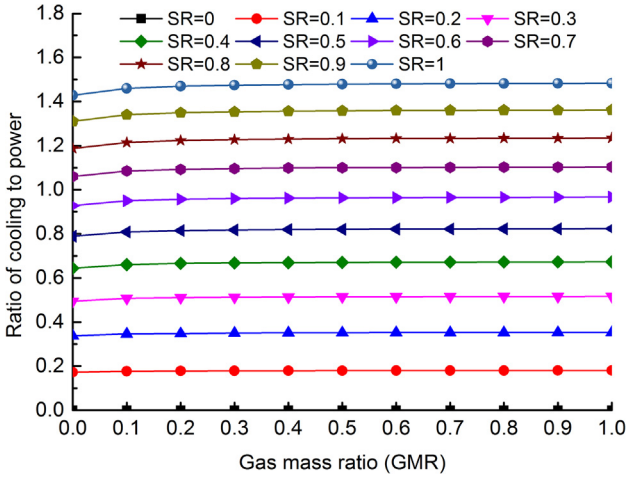

Fig. 8. The influences of split ratio and gas mass ratio on the ratio of cooling to power.

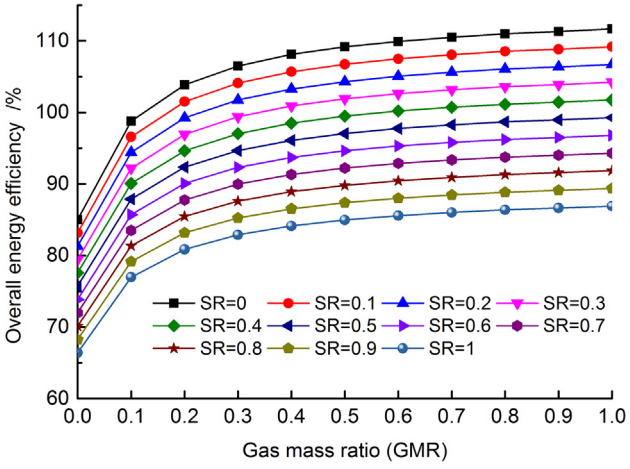

Fig. 9. The influences of split ratio and gas mass ratio on overall energy efficiency of proposed system.

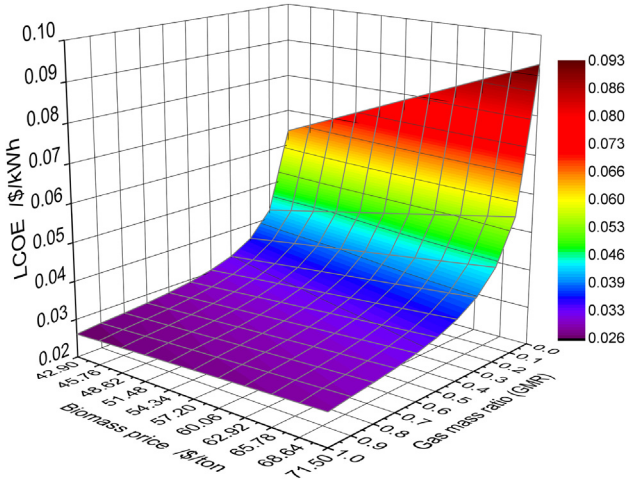

Fig. 10. The variations of levelized cost of energy at different biomass price and gas mass ratio.

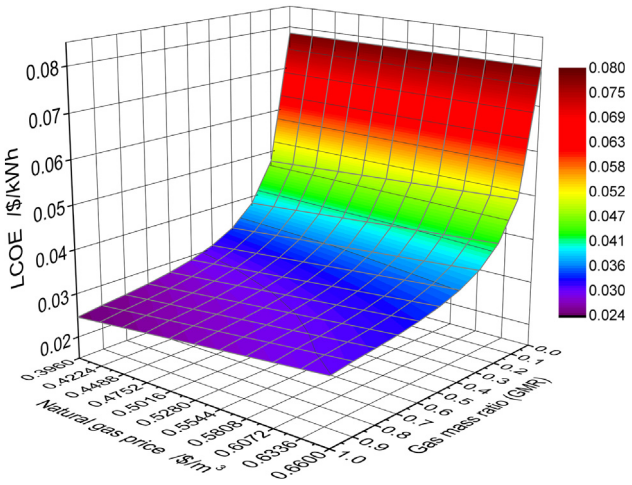

Fig. 11. The variations of levelized cost of energy at different natural gas price and gas mass ratio.

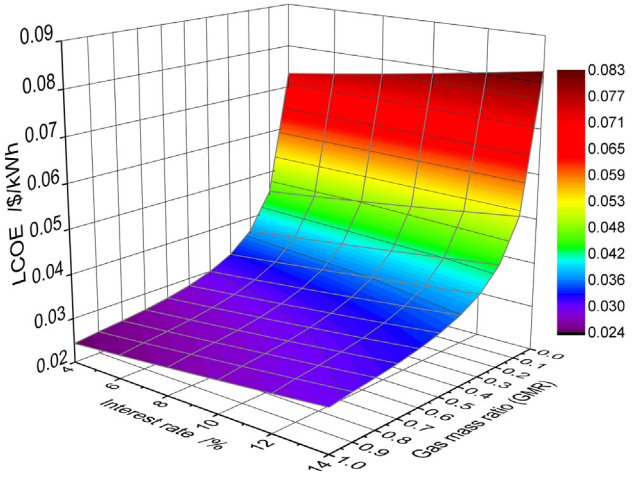

Fig. 12. The variations of levelized cost of energy at different interest rate and gas mass ratio.

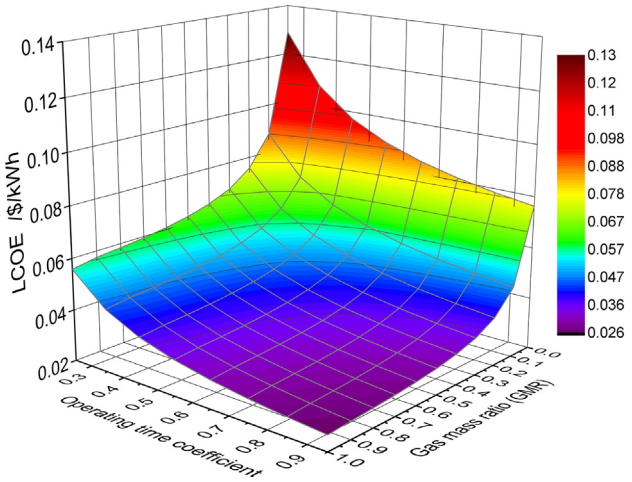

Fig. 13. The variations of levelized cost of energy at different operating time coefficient and gas mass ratio.

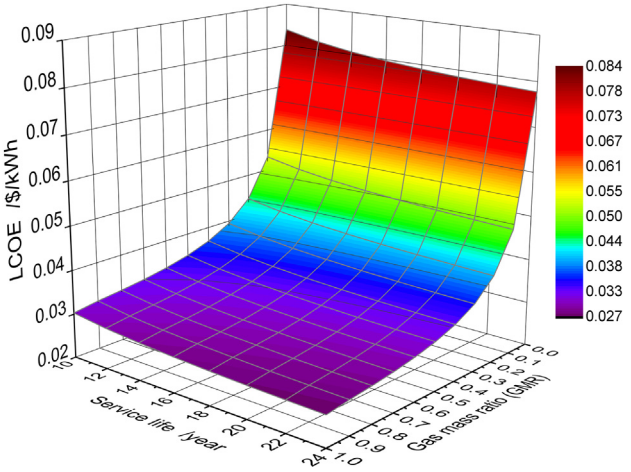

Fig. 14. The variations of levelized cost of energy at different service life and gas mass ratio.

decreases with the increase in service life, and the annual total cost of proposed system decreases accordingly. Therefore, it results in the decrease of levelized cost of energy.

6. Conclusion

In this study, a novel combined cooling, heating and power (CCHP) system integrating with biomass, natural gas and geothermal energy, which mainly consists of an air-biomass gasification subsystem, steam turbine electricity generation subsystem, gas turbine electricity generation subsystem, waste heat utilization subsystem and ground source heat pump subsystem, is proposed, the thermodynamic and economic performances of proposed CCHP system are investigated. The effects of key parameters (such as gas mass ratio, flue gas split ratio) on system performances are performed, besides that the sensitivity analysis of some economic factors (biomass price, natural gas price, interest rate, operating time coefficient and service life) are also studied. The main research findings can be illustrated as follows:

(1) The introduction of natural gas contributes to improve the reliability of energy supply system, and increase the energy density of inputs in prime mover. The LHV of mixture gas increases from 3.94 MJ/kg to 26.98 MJ/kg with the increase in gas mass ratio from 0 to 1.0, when the flow rate of biomass keeps constant. On the other hand, the introduction of geothermal energy increases the heating output of proposed system.
(2) The gas mass ratio and flue gas split ratio have a significant effect on system performances. The electricity, heating and cooling generated by proposed system all increase with the increase in gas mass ratio. With the increase in flue gas split ratio, the electricity and cooling increase, on the contrary, the heating output decreases owing to the decreasing of flue gas in HX. For the overall energy efficiency, it increases with the increase in split ratio and gas mass ratio, and the increasing range of overall energy efficiency decreases when the gas mass ratio exceeds 0.4.
(3) The sensitivity analysis of some economic factors on system performances is also performed. The increase in biomass price, natural gas price and interest rate lead to an increase of levelized cost of energy, the levelized cost of energy decreases with the increasing of operating time coefficient and service life. Moreover, the levelized cost of energy decreases exponentially with the increase in gas mass ratio. Therefore, in terms of levelized cost of energy reduction the gas mass ratio can't be too low.
(4) In the case study, when the gas mass ratio and flue gas split ratio are set at 0.5 and 0.5, respectively, the electricity, heating and cooling output is calculated to 4154 kW, 5489 kW, 3408 kW, respectively. The overall energy efficiency of proposed CCHP system can reach at 97.05%, and the levelized cost of energy is 0.0315 $/kWh.

In general, the proposed novel CCHP system based on biomass, natural gas and geothermal energy realizes the coupling utilization between renewable energy and fossil fuel, which provides a promising approach for novel energy integrated system.

Acknowledgements

This study is supported by the National Natural Science Foundation of China (NO. 51541603), Natural Science Foundation of Hunan Province (NO. 2016JJ2021), Science Research Foundation of Education Bureau of Hunan Province (NO. 16C0057) and the International Science & Technology Cooperation Program of China (NO. 2014DFE70230).

Appendix A. Investment cost function of component [36,41,42]

Gasifier:

$$C_{gasifier} = 1600(\dot{m}_{biomass}\ [\mathrm{kg/h}])^{0.67}$$

HX-01:

$$C_{HX-01} = 130\left(\frac{A_{HX-01}}{0.093}\right)^{0.78}$$

HX-02:

$$C_{HX-02} = 130\left(\frac{A_{HX-02}}{0.093}\right)^{0.78}$$

Steam turbine:

$$C_{steam\ turbine} = N_{11} W_{steam\ turbine}^{0.7}\left(1 + \left(\frac{0.05}{1-\eta_{is,steam\ turbine}}\right)^{3}\right)\cdot\left(1 + 5\cdot\exp\left(\frac{T_{in}-866}{10.42}\right)\right)$$

$$N_{11} = 3880.5\ \mathrm{kW}^{-0.7}$$

Condenser-01:

$$C_{condenser-01} = 8000\left(\frac{A_{condenser-01}}{100}\right)^{0.6}$$

Pump-01:

$$C_{pump-01} = 800\left(\frac{W_{pump-01}}{10}\right)^{0.26}\left(\frac{1-\eta_{pump-01}}{\eta_{pump-01}}\right)^{0.5}$$

GCU:

$$C_{GCU} = 0.05 \times 1600(\dot{m}_{biomass}\ [\mathrm{kg/h}])^{0.67}$$

Bio-gas compressor:

$$C_{bio-gas\ compressor} = \frac{N_{21}\dot{m}_{bio-gas}}{N_{22}-\eta_{is,bio-gas\ compressor}} r_p \ln(r_p)$$

$N_{21} = 71.1$ \$/(kg/s) $N_{22} = 0.9$

Gas mixer:

$$C_{gas\ mixer} = 0$$

Combustor:

$$C_{combustor} = \frac{N_{31}\dot{m}_{air}}{N_{32}-0.98}(1 + \exp(N_{33}T_{combustor}-N_{34}))$$

$N_{31} = 46.08$ $N_{32} = 0.995$ $N_{33} = 0.018$ $N_{34} = 26.4$

Gas turbine:

$$C_{gas\ turbine} = \frac{N_{41}\dot{m}_{23}}{N_{42}-\eta_{is,GT}} \ln\left(\frac{P_8}{P_9}\right)(1 + \exp(N_{43}T_8-N_{44}))$$

$N_{41} = 479.34$ $N_{42} = 0.92$ $N_{43} = 0.036$ $N_{44} = 54.4$

Air compressor:

$$C_{air\ compressor} = \frac{N_{51}\dot{m}_{air}}{N_{52}-\eta_{is,air\ compressor}} r_p \ln(r_p)$$

$N_{51} = 71.1$ \$/(kg/s) $N_{52} = 0.9$

Recuperator:

$$C_{recuperator} = 130\left(\frac{A_{recuperator}}{0.093}\right)^{0.78}$$

Splitter:

$$C_{splitter} = 0$$

Absorption chiller:

$$C_{absorption\ chiller} = 196 \times Q_{absorption\ chiller}$$

HX:

$$C_{HX} = 130\left(\frac{A_{HX}}{0.093}\right)^{0.78}$$

Condenser:

$$C_{condenser} = 8000\left(\frac{A_{condenser}}{100}\right)^{0.6}$$

Compressor:

$$C_{compressor} = \frac{N_{61}\dot{m}_{refrigerant}}{N_{62}-\eta_{is,compressor}} r_p \ln(r_p)$$

$N_{61} = 39.5$ \$/(kg/s) $N_{62} = 0.9$

Evaporator:

$$C_{evaporator} = 16000\left(\frac{A_{evaporator}}{100}\right)^{0.6}$$

Throttle valve:

$$C_{throttle\ valve} = 0$$

Pump-02:

$$C_{pump-02} = 800\left(\frac{W_{pump-02}}{10}\right)^{0.26}\left(\frac{1-\eta_{pump-02}}{\eta_{pump-02}}\right)^{0.5}$$

References

[1] IEA. Global energy and CO2 status report; 2017. < http://www.iea.org/statistics/ > .
[2] Han J, Ouyang L, Xu Y, et al. Current status of distributed energy system in China. Renew Sustain Energy Rev 2016;55:288–97.
[3] Prando D, Renzi M, Gasparella A, et al. Monitoring of the energy performance of a district heating CHP plant based on biomass boiler and ORC generator. Appl Therm Eng 2015;79:98–107.
[4] Jing R, Wang M, Brandon N, et al. Multi-criteria evaluation of solid oxide fuel cell based combined cooling heating and power (SOFC-CCHP) applications for public buildings in China. Energy 2017;141:273–89.
[5] Wang J, Li M, Ren F, et al. Modified exergoeconomic analysis method based on energy level with reliability consideration: cost allocations in a biomass trigeneration system. Renew Energy 2018;123:104–16.
[6] Sahoo U, Kumar R, Pant PC, et al. Development of an innovative polygeneration process in hybrid solar-biomass system for combined power, cooling and desalination. Appl Therm Eng 2017;120:560–7.
[7] Wang J, Yang Y. Energy, exergy and environmental analysis of a hybrid combined cooling heating and power system utilizing biomass and solar energy. Energy Convers Manage 2016;124:566–77.
[8] Khalid F, Dincer I, Rosen MA. Techno-economic assessment of a solar-geothermal multigeneration system for buildings. Int J Hydrogen Energy 2017;42(33):21454–62.
[9] Bornapour M, Hooshmand RA, Khodabakhshian A, et al. Optimal coordinated scheduling of combined heat and power fuel cell, wind, and photovoltaic units in micro grids considering uncertainties. Energy 2016;117:176–89.
[10] Zhang B, Liu QB, Jing L, et al. A polygeneration system for the methanol production and the power generation with the solar-biomass thermal gasification. Energy Convers Manage 2014;61:1561–4.
[11] Ellabban O, Abu-Rub H, Blaabjerg F. Renewable energy resources: current status, future prospects and their enabling technology. Renew Sustain Energy Rev 2014;39(2):748–64.
[12] Couto N, Silva V, Monteiro E, et al. Modeling of fluidized bed gasification: assessment of zero-dimensional and CFD approaches. J Therm Sci 2015;24(4):378–85.
[13] Song G, Feng F, Xiao J, et al. Technical assessment of synthetic natural gas (SNG) production from agriculture residuals. J Therm Sci 2013;22(4):359–65.
[14] Andersson J, Lundgren J, Marklund M. Methanol production via pressurized entrained flow biomass gasification - techno-economic comparison of integrated vs. stand-alone production. Biomass Bioenergy 2014;64(5):256–68.
[15] Bai Z, Liu Q, Lei J, et al. New solar-biomass power generation system integrated a two-stage gasifier. Appl Energy 2017;194:310–9.
[16] Liu L, Zhu N, Zhao J. Thermal equilibrium research of solar seasonal storage system coupling with ground-source heat pump. Energy 2016;99:83–90.
[17] Malik M, Dincer I, Rosen MA. Development and analysis of a new renewable energy-based multi-generation system. Energy 2015;79:90–9.
[18] Patarau T, Petreus D, Etz R. Analysis and optimization of a geothermal, biomass, solar hybrid system: an application of PV*Sol software. Int Spring Seminar Electron Technol IEEE 2015:370–5.
[19] Seethamraju S, Eisenberg D, Seifkar Navid, et al. Simulation-based study of a novel integration: geothermal-biomass power plant. Energy Fuels 2014;28(12):7632–42.
[20] Moret S, Peduzzi E, Gerber L, et al. Integration of deep geothermal energy and woody biomass conversion pathways in urban systems. Energy Convers Manage 2016;129:305–18.
[21] Lukawski MZ, Vilaetis K, Gkogka L, et al. A proposed hybrid geothermal-natural gas-biomass energy system for cornell university. Technical and economic assessment of retrofitting a low-temperature geothermal district heating system and heat cascading solutions. The 38th Workshop on geothermal reservoir engineering proceedings. Stanford (CA, USA): Stanford University; 2013.
[22] Zhang X, Li H, Liu L, et al. Exergetic and exergoeconomic assessment of a novel CHP system integrating biomass partial gasification with ground source heat pump. Energy Convers Manage 2018;156:666–79.
[23] Zhang X, Li H, Liu L, et al. Optimization analysis of a novel combined heating and power system based on biomass partial gasification and ground source heat pump. Energy Convers Manage 2018;163:355–70.
[24] Fan J, Hong H, Zhu L, et al. Thermodynamic and environmental evaluation of biomass and coal co-fuelled gasification chemical looping combustion with CO_2 capture for combined cooling, heating and power production. Appl Energy 2017;195:861–76.
[25] Walter A, Llagostera J, Frangopoulos CA, et al. Feasibility analysis of co-fired combined-cycles using biomass-derived gas and natural gas. Energy Convers Manage 2007;48(11):2888–96.
[26] Wang J, Mao T, Sui J, et al. Modeling and performance analysis of CCHP (combined cooling, heating and power) system based on co-firing of natural gas and biomass gasification gas. Energy 2015;93:801–15.
[27] Agbor E, Oyedun AO, Zhang X, et al. Integrated techno-economic and environmental assessments of sixty scenarios for co-firing biomass with coal and natural gas. Appl Energy 2016;169:433–49.
[28] Fiaschi D, Carta R. CO_2 abatement by co-firing of natural gas and biomass-derived gas in a gas turbine. Energy 2007;32(4):549–67.
[29] Nikpey H, Assadi M, Breuhaus P, et al. Experimental evaluation and ANN modeling of a recuperative micro gas turbine burning mixtures of natural gas and biogas. Appl Energy 2014;117(117):30–41.
[30] Kang JY, Kang DW, Tong SK, et al. Economic evaluation of biogas and natural gas co-firing in gas turbine combined heat and power systems. Appl Therm Eng 2014;70(1):723–31.
[31] Puig-Arnavat M, Bruno JC, Coronas A. Review and analysis of biomass gasification models. Renew Sustain Energy Rev 2010;14(9):2841–51.
[32] Zhang X, Li H, Liu L, et al. Thermodynamic and economic analysis of biomass partial gasification process. Appl Therm Eng 2018;129:410–20.
[33] Li H, Zhang X, Liu L, et al. Exergy and environmental assessments of a novel trigeneration system taking biomass and solar energy as co-feeds. Appl Therm Eng 2016;104:697–706.
[34] Li HQ, Kang SS, Yu Z, et al. A feasible system integrating combined heating and power system with ground-source heat pump. Energy 2014;74(5):240–7.
[35] Mosaffa AH, Farshi LG. Thermodynamic and economic assessments of a novel CCHP cycle utilizing low-temperature heat sources for domestic applications. Renew Energy 2018;120:134–50.
[36] Soltani S, Mahmoudi SMS, Yari M, et al. A comparative exergoeconomic analysis of two biomass and co-firing combined power plants. Energy Convers Manage 2013;76:83–91.
[37] Li M, Jiang XZ, Zheng D, et al. Thermodynamic boundaries of energy saving in conventional CCHP (Combined Cooling, Heating and Power) systems. Energy 2016;94:243–9.
[38] Nižetić S, Duić N, Papadopulos AM, et al. Energy efficiency evaluation of a hybrid energy system for building applications in a Mediterranean climate and its feasibility aspect. Energy 2015;90:1171–9.
[39] Neyer D, Ostheimer M, Dipasquale C, et al. Technical and economic assessment of solar heating and cooling – methodology and examples of IEA SHC Task 53. Sol Energy 2018.
[40] Jing R, Wang M, Wang W, et al. Economic and environmental multi-optimal design and dispatch of solid oxide fuel cell based CCHP system. Energy Convers Manage 2017;154:365–79.
[41] Khanmohammadi S, Atashkari K, Kouhikamali R. Exergoeconomic multi-objective optimization of an externally fired gas turbine integrated with a biomass gasifier. Appl Therm Eng 2015;91:848–59.
[42] Khani L, Mahmoudi SMS, Chitsaz A, et al. Energy and exergoeconomic evaluation of a new power/cooling cogeneration system based on a solid oxide fuel cell. Energy 2016;94:64–77.